Published in final edited form as:
Biochim Biophys Acta. 2010 February ; 1802(2): 275–283. doi:10.1016/j.bbadis.2009.10.005.

A SUGGESTED ROLE FOR MITOCHONDRIA IN NOONAN SYNDROME

Icksoo Lee[a], **Alena Pecinova**[a], **Petr Pecina**[a], **Benjamin G. Neel**[b], **Toshiyuki Araki**[b], **Raju Kucherlapati**[c], **Amy E. Roberts**[d], and **Maik Huttemann**[*,a]

[a] Center forMolecular Medicine and Genetics, Wayne State University School of Medicine, Detroit, Michigan 48201, USA

[b] Ontario Cancer Institute, Toronto, Canada

[c] Harvard Medical School, Boston, USA

[d] Children's Hospital Boston, Boston, USA

Abstract

Noonan syndrome (NS) is an autosomal dominant disorder, and a main feature is congenital heart malformation. About 50% of cases are caused by gain of function mutations in the tyrosine phosphatase SHP2/*PTPN11*, a downstream regulator of ERK/MAPK. Recently it was reported that SHP2 also localizes to the mitochondrial intercristae/intermembrane space (IMS), but the role of SHP2 in mitochondria is unclear. The mitochondrial oxidative phosphorylation (OxPhos) system provides the vast majority of cellular energy and produces reactive oxygen species (ROS). Changes in ROS may interfere with organ development such as that observed in NS patients. Several phosphorylation sites have been found in OxPhos components including cytochrome *c* oxidase (CcO) and cytochrome *c* (Cyt*c*), and we hypothesized that OxPhos complexes may be direct or indirect targets of SHP2. We analyzed mitochondrial function using mouse fibroblasts from wild-types, SHP2 knockdowns, and D61G SHP2 mutants leading to constitutively active SHP2, as found in NS patients. Levels of OxPhos complexes were similar except for CcO and Cyt*c*, which were 37% and 28% reduced in the D61G cells. However, CcO activity was significantly increased, as we also found for two lymphoblast cell lines from NS patients with two independent mutations in *PTPN11*. D61G cells showed lower mitochondrial membrane potential and 30% lower ATP content compared to controls. ROS were significantly increased, aconitase activity, a marker for ROS-induced damage, was decreased, and catalase activity was increased in D61G cells. We propose that decreased energy levels and/or increased ROS may explain, at least in part, some of the clinical features in NS that overlap with children with mitochondrial disorders.

Keywords

cardio-facio-cutaneous syndrome; cytochrome *c* oxidase; Noonan syndrome; mitochondria; oxidative phosphorylation; *PTPN11*; reactive oxygen species; SHP2

[*]To whom correspondence should be addressed: Center for Molecular Medicine and Genetics, Wayne State University School of Medicine, 3214 Scott Hall, 540 E. Canfield, Detroit, MI 48201, USA, Fax: (+1) 313-577-5218, Telephone: (+1) 313-577-9150, mhuttema@wayne.edu.

1. Introduction

SHP2 is a ubiquitously expressed non-receptor protein tyrosine phosphatase (PTP) [1]. SHP2 is involved in several cellular processes including cell development, growth, and survival, and it is thus a central player in important signaling pathways, including mitogen-activated protein kinases (MAPK) and Janus-tyrosine kinase 2 (Jak2)/signal transducer and activator of transcription (STAT) signaling [2]. SHP2 is encoded by the gene *PTPN11* and contains two N-terminal Src-homology 2 (SH2) domains and a central tyrosine phosphatase domain. The C-terminal region contains two regulatory tyrosine phosphorylation sites required for full downstream activation of the MAPK pathway via fibroblast growth factor-, platelet-derived growth factor-, but not epidermal growth factor-triggered signaling [3]. Mice homozygous for dysfunctional SHP2, which lack the N-terminal SH2 domain required for phospho-tyrosine recognition but with a functional phosphatase domain, die before E.11.5 of gestation [4], whereas PTPN11 null mice die significantly earlier during the peri-implantation period [5].

Mutations in *PTPN11* can cause Noonan syndrome (NS), the related LEOPARD syndrome, and leukemia. NS mutations usually lead to constitutively active SHP2. For example, the NS-causing mutation D61G results in about 10-fold increased basal SHP2 activity, whereas the leukemia causing D61Y mutation leads to an about 20-fold increased basal activity [6]. With an incidence of 1:1,000 to 1:2,500 live births, NS is a common cause of congenital heart disease. NS features include heart abnormalities, short stature, characteristic facies, hypotonia, developmental delay, learning problems, and leukemia predisposition. Gain-of-function mutations in *PTPN11* cause approximately 50% of Noonan syndrome cases [7]. Mutations in other genes that are part of the MAPK pathway have also been identified in NS patients, such as gain-of-function mutations in the RAS guanine nucleotide-exchange factor SOS1, which account for approximately 10% of NS cases [8].

In addition to being a central constituent of receptor tyrosine kinase signaling near the plasma membrane, SHP2 was recently reported to also localize to mitochondria derived from rat brain [9,10], specifically to the intercristae/intermembrane space (IMS). A possible direct or indirect substrate of SHP2 is a central unit of enzymes that is housed in the inner mitochondrial membrane, the oxidative phosphorylation (OxPhos) machinery. It consists of the electron transport chain (ETC) and ATP synthase. The ETC is a series of electron transferring moieties consisting of NADH dehydrogenase (complex I), succinate dehydrogenase (SDH; complex II), ubiquinone, bc_1-complex (complex III), cytochrome *c* (Cyt*c*), and cytochrome *c* oxidase (CcO; complex IV). Electron transport in the ETC complexes I, III, and IV is coupled to proton pumping, which generates the mitochondrial proton membrane potential Ψ_m across the inner mitochondrial membrane. $\Delta\Psi_m$ is utilized by ATP synthase (complex V) to synthesize ATP from ADP and phosphate via the backflow of protons from the mitochondrial IMS to the matrix. Through aerobic respiration, OxPhos is responsible for more than 90% of cellular energy production. In addition, it is a major producer of reactive oxygen species (ROS). Since a lack of energy and/or increased ROS are increasingly associated with numerous human diseases, we hypothesized that mutations of SHP2 as found in NS may affect mitochondrial function. In addition, ROS are involved in cell signaling and perturbations of ROS levels might contribute to organ maldevelopment as found in NS patients.

Recently, new models have been presented to explain the regulation of mitochondrial energy and ROS production. In the traditional view, which is mainly based on studies in bacteria, the activity of the ETC proton pumps is regulated by the mitochondrial membrane potential $\Delta\Psi_m$, which at high levels inhibits further proton pumping. The Kadenbach group has shown that CcO is allosterically regulated by the ATP/ADP ratio, a measure of cellular energy demand, and the group proposed that this regulation is a $\Delta\Psi_m$-independent mechanism to maintain lower $\Delta\Psi_m$ levels in higher organisms [11]. Maintenance of lower $\Delta\Psi_m$ levels makes sense since

ROS are excessively produced at high mitochondrial membrane potentials [12]. In addition to allosteric regulation we and others have proposed that post-translational modifications, specifically reversible phosphorylation, may play an essential role in the regulation of OxPhos and $\Delta\Psi_m$. However, very little is known about the effect of cell signaling pathways on OxPhos. Nineteen phosphorylation sites have been mapped in mammalian OxPhos complexes and Cyt*c*, but signaling pathways including the immediate upstream kinases and phosphatases involved in these posttranslational modifications remain unknown in most instances (for recent reviews see [13,14]). Among those phosphorylation sites identified are five tyrosine residues: Y75 of the δ-subunit of ATP synthase [15], which is located in the mitochondrial matrix as is Y11 of CcO subunit IV [16], and Y304 of CcO catalytic subunit I [17,18], Cyt*c* Y48 [19], and Cyt*c* Y97 [20], which are accessible from and located in the IMS as is SHP2. CcO Y304, Cyt*c* Y48, and Cyt*c* Y97 phosphorylation leads to an inhibition of enzyme activity, and dephosphorylation of any of these sites would lead to increased respiration.

We here show that CcO activity is significantly increased in lymphoblast cell lines from NS patients, as well as in mouse embryonic fibroblasts (MEFs) containing the NS-causing mutation D61G. Using the latter cell line we show that CcO and Cyt*c* are downregulated at the protein level in contrast to the other OxPhos complexes. ATP levels are lower in D61G cells compared to controls and ROS are increased, which is also reflected in increased mitochondrial damage and changes of ROS scavenging enzymes. We discuss these findings in light of alterations of energy and ROS as a possible contributor to the pathology of NS.

2. Materials and methods

2.1. Cell lines

Epstein Barr virus transformed human lymphoblast (B-cell) lines from two control and two NS patients with mutations in SHP2 (patient 1: A317C, Asp106→Ala; patient 2: A922G, Asn308→Asp) were grown in DMEM media supplemented with 15% fetal bovine serum (FBS) and 1x penicillin/streptomycin/L-glutamine (Invitrogen) at 37°C in a 5% CO_2 atmosphere. Mouse embryonic fibroblasts (MEFs) derived from wild-type mice (WT), D61G mutant mice, and SHP2 knockdown mice lacking exon 3 ($Ex3^{-/-}$; knockdown, KD) have been extensively characterized in the past [21–23] and were cultured in DMEM media supplemented as above.

2.2. Western blot analysis

Cultured cells were washed with PBS and collected by trypsinization. The cells were denatured in SDS-polyacrylamide gel electrophoresis (SDS-PAGE) sample buffer for 40 min at room temperature under shaking. SDS-PAGE was carried out using a 10% acrylamide Tris/glycine/SDS gel system. After gel electrophoresis, proteins were transferred to a PVDF membrane (0.2 mm, Bio-Rad, Hercules, CA) using transfer buffer (25 mM Tris base, 192 mM glycine, 20% methanol and 0.01% SDS) for 60 min at 25V. The membrane for Cyt*c* detection was UV-cross linked (Stratagene, UV Stratalinker 1800, 240 mjoules) before blocking to enhance the retention of Cyt*c* on the membrane. The membrane was blocked in 10% non fatdry milk (NFDM)/PBS overnight at 4°C without shaking. The membrane was washed with PBS for 5min and incubated with primary antibodies for 2 h at room temperature under shaking. The dilution conditions for primary antibodies are as follows. 1:2,000 dilution in PBS-Tween 20 (0.1%): anti-Cyt*c* (556433, BD Pharmingen), anti-MnSOD (ab13534, Abcam, Cambridge, MA) and anti-GAPDH (G8795, Sigma-Aldrich, St. Louis, MO); 1:5,000 dilution in PBS-Tween 20 (0.1%): anti-OxPhos complex I NDUFB6 subunit (MS108, MitoSciences, Eugene, OR), anti-OxPhos complex III subunit core I (MS303, MitoSciences), anti-OxPhos complex IV subunit I (MS404, MitoSciences), anti-OxPhos complex V α subunit (MS502, MitoSciences), and anti-porin (MSA03, MitoSciences); 1:8,000 dilution in PBS-Tween 20

(0.1%): anti-β actin (4970, Cell Signaling Technology, Danvers, MA); 1:1,000 dilution in 5% NFDM/PBS-Tween 20 (0.1%): anti-OxPhos complex II subunit 70 kDa Fp (MS204, MitoSciences), and anti-CuZnSOD (574597, Calbiochem, Madison, WI); 1:200 dilution in 5% NFDM/PBS-Tween 20 (0.1%): anti-GPx-1 (sc-22145, Santa Cruz Biotechnology, Santa Cruz, CA). The membranes were washed in PBS-Tween 20 (0.1%) two times for 10 min. The dilution conditions for secondary antibodies are the following. 1:5,000 dilution of anti-mouse IgG-horse radish peroxidase (HRP) conjugated (GE Healthcare, Piscataway, NJ) in PBS-Tween 20 (0.1%): anti-OxPhos complex I NDUFB6 subunit, anti-OxPhos complex III subunit core I, anti-OxPhos complex IV subunit I, anti-OxPhos complex V subunit α, and anti-porin, anti-Cyt*c*; 1:7,000 dilution of anti-mouse IgG-HRP conjugated in PBS-Tween 20 (0.1%): anti-GAPDH; 1:5,000 dilution of anti-rabbit IgG-HRP conjugated (GE Healthcare) in PBS-Tween 20 (0.1%): anti-MnSOD; 1:8,000 dilution of anti-rabbit IgG-HRP conjugated in PBS-Tween 20 (0.1%): anti-β actin; 1:5,000 dilution of anti-mouse IgG-HRP conjugated in 5% NFDM/PBS-Tween 20 (0.1%): Anti-OxPhos complex II subunit 70 kDa Fp; 1:5,000 dilution of anti-sheep IgG-HRP conjugated (Santa Cruz) in 5% NFDM/PBS-Tween 20 (0.1%): anti-CuZnSOD. The membranes were incubated with antibodies for 1 h at room temperature under shaking and washed in PBS-Tween 20 (0.1%) two times for 10 min. Signals were detected by the chemiluminescence method (ECL^+ kit, GE Healthcare), and band intensities were quantified using the program Image Quant vers. 5.1 (Molecular Dynamics, Sunnyvale, CA).

2.3. CcO activity measurements

CcO activity was analyzed in a closed 200 μL chamber equipped with a micro Clark-type oxygen electrode (Oxygraph system, Hansatech). Cultured cells were washed with phosphate buffered saline (PBS), harvested by scraping in the presence of 10 mL PBS, collected by centrifugation (500 × g, 5 min), washed once more with PBS, and sonicated as described [18]. Measurements were performed in measuring buffer (10 mM K-HEPES (pH 7.4), 40 mM KCl, 1% Tween 20, 2 μM oligomycin, 1 mM PMSF, 10 mM KF, 2 mM EGTA) in the presence of 20 mM ascorbate and increasing amounts of cow heart Cyt*c*. Oxygen consumption was recorded on a computer and analyzed with the Oxygraph software. Protein concentration was determined with the DC protein assay kit (Bio-rad). CcO activity is defined as consumed O_2 (μM)/(min total protein (mg)).

2.4 Mitochondrial membrane potential measurements

The mitochondrial membrane potential of intact cells was measured as described [24] with modifications. Cultured cells were washed with PBS and trypsinized. The concentration of cells was adjusted to 0.2 mg/mL protein with DMEM media without phenol red (21063, Gibco-Invitrogen, Carlsbad, CA) and not supplemented with fetal bovine serum and antibiotics. 20 nM tetramethylrhodamine-methylester (TMRM, T-668, Molecular Probes-Invitrogen) was added to the cell suspension. As a control, the mitochondrial membrane potential was dissipated using 1 μM carbonyl cyanide 4-(trifluoromethoxy) phenylhydrazone (FCCP). The sample was incubated at 37°C for 30 min in the dark under slow rotation (e.g., in a hybridization oven). Yellow fluorescence (excitation 532 nm laser; emission, 585 nm, band pass, 42 nm) was measured using a BD FACS Array (BD Biosciences, San Jose, CA), and data were analyzed with WinMDI vers. 2.9 software. The TMRM fluorescence was normalized to fluorescence of MitoTracker Red CMXRos (M-7512, Molecular probes-Invitrogen). MitoTracker Red accumulates in fibroblast mitochondria in a membrane potential-independent manner. Conditions for treatment and measurement of the cells were identical to experiments with TMRM, except the cells were incubated with 30 nM MitoTracker Red instead.

2.5. Spectrophotometric measurement of citrate synthase activity

Citrate synthase (CS) activity was analyzed by a spectrophotometric assay as described [25]. Briefly, 0.1 mg of cells were solubilized with 0.1% of dodecyl maltoside in media containing 100 mM Tris-Cl (pH 8.1), 0.1 mM dithionitrobenzoic acid, and 50 μM acetyl-CoA. The reaction was started with 0.5 mM oxaloacetic acid and changes of absorbance at 412 nm were read for 1 minute. Enzyme activity was calculated from the absorbance data using an extinction coefficient of ε_{412}=13.6 $mM^{-1}cm^{-1}$.

2.6. Bioluminescent determination of ATP concentrations

Cultured cells were collected by scraping and immediately stored in aliquots at −80°C until measurement. ATP was released using the boiling method by addition of 300 μL boiling buffer (100 mM Tris-Cl (pH 7.75), 4 mM EDTA) and immediate transfer to a boiling water bath for 2 min. Samples were put on ice, sonicated, and diluted 100 fold. Fifty μL were used to determine the ATP concentration using the ATP biolumescence assay kit HS II (Roche) according to the manufacturer's protocol. Experiments were performed in triplicates and data were standardized to the protein concentration using the DC protein assay kit (Bio-rad).

2.7. Reactive oxygen species measurements

Cells were trypsinized, collected by centrifugation, washed as above, and incubated with the ROS-sensitive probe 2′,7′-dichlorodihydrofluorescein diacetate (H_2DCFDA; D-399, Molecular Probes) at a final concentration of 7.5 μM for 20 min at 37°C in the dark. Cells were collected by centrifugation, supplemented with media and incubated in the dark for 20 min at 37°C. As a control, cells were incubated in the presence of 100 μM H_2O_2. Cells were collected by centrifugation, resuspended in PBS, transferred to a 96-well plate (Costar 3603; 200 μL per well), and analyzed on an Ascent Fluoroskan plate reader (488 nm excitation; 527 nm emission) as described [26]. Experiments were performed in triplicates and data standardized to the protein concentration determined as above.

2.8. Aconitase activity measurements

The aconitase activity was measured as a parameter of oxidative damage in cells according to Bulteau *et al.* [27] with several modifications. Aconitase catalyzes citrate to isocitrate and the isocitrate is subsequently decarboxylated to α-ketoglutarate by isocitrate dehydrogenase. NADPH is a byproduct of the latter process and the rate of NADPH production was measured at 340 nm using a spectrophotometer (Jasco V-570). Cultured cells were washed with PBS, collected by trypsinization, and kept on ice until the assay was performed. Cells were diluted to 2.5 mg/mL final protein concentration in solubilization buffer (25 mM KH_2PO_4 (pH 7.25), 2 mM $MnCl_2$, 0.1% dodecyl maltoside) and incubated at room temperature for 2 min. The sample was centrifuged (14,000 rpm for 2 min) and the supernatant was transferred to a quartz cuvette. Isocitrate dehydrogenase (4.25 U/mL, Sigma, I2002) and $NADP^+$ (2 mM) were added and mixed. NADPH production was monitored at 340 nm for 5 min by addition of 1 mM sodium citrate. Basal NADPH production due to the endogenous citrate was measured without addition of sodium citrate at 340 nm for 5 min and subtracted from the experimental data. The NADPH concentration was calculated using extinction coefficient $\varepsilon_{340\ nm}$ = 6.22 $mM^{-1}cm^{-1}$.

2.9. Catalase activity measurements

Catalase activity was measured as described [28] with modifications. Degradation of H_2O_2 by catalase was monitored spectrophotometrically at 240 nm as catalase activity. The cultured cells were washed with PBS, collected by trypsinization and kept on ice until the assay was performed. The cells were solubilized to 0.4mg/ml protein concentration in 50 mM KH_2PO_4 (pH 7.25), 0.1% dodecylmatoside at room temperature for 2 min. The sample was centrifuged

at 14,000 rpm for 2min and the supernatant was transferred to a quartz cuvette. The absorbance at 240 nm was monitored for 3 min after the addition of H_2O_2 to a final concentration of 8.82 mM. The decrease of H_2O_2 was determined using an extinction coefficient of $\varepsilon_{240\ nm} = 43.6\ M^{-1}cm^{-1}$. Basal absorbance at 240 nm was measured at the end of the assay by addition of NaN_3, which inhibits catalase, and subtracted from the experimental data.

2.10. Statistical Analysis

Data are presented as mean ± standard error of the mean (SEM). One-way analysis of variance (ANOVA) was used to determine statistical significance between groups.

3. Results

3.1. Cytochrome c oxidase activity is increased in lymphoblast cell lines derived from Noonan patients and mouse fibroblasts carrying the Noonan syndrome-causing Asp61 to Gly (D61G) mutation

Since SHP2 also localizes to the mitochondrial IMS, OxPhos complexes may be direct or indirect targets of SHP2. CcO is a possible direct target of SHP2 since we and others have shown that it can be tyrosine phosphorylated on the IMS side on tyrosine 304 of subunit I [17,18] and on a yet to be mapped tyrosine residue of subunit II [29]. CcO subunits III and IV may also contain additional phosphorylated tyrosine residues located on the IMS side since very strong signals were obtained with a phosphotyrosine-specific antibody using isolated CcO [16].

Initially, we used human lymphoblast cell lines from two patients with NS caused by mutations in SHP2. Patient 1 has a A317C transversion leading to the change of aspartate 106 to alanine, which is located in the linker domain between the N- and C-terminal SH2 domains of SHP2. This patient had some features also reported in children with mitochondrial disorder including growth delay, developmental delays attributed to hypotonia, short stature, and ptosis, Patient 2 has a A922G transition causing a change of asparagine 308 to aspartate, which is located in the protein tyrosine phosphatase domain. This patient also had some features reported in children with mitochondrial disorder including failure to thrive and short stature. In comparison to the controls, CcO activity was 116% and 74% increased at saturating substrate Cyt*c* concentrations in patients 1 and 2, respectively (Fig. 1A, compare closed and open symbols). At lower and intermediate Cyt*c* concentrations CcO activity was up to threefold increased in both patient cell lines compared to the controls.

Consistent with the above finding, similar results were obtained with mouse embryonic fibroblast (MEF) cells containing the NS-causing D61G mutation, which showed 63% increased CcO activity compared to controls (Fig. 1B). For this study we also included SHP2 knockdown cells lacking exon 3 as an additional control. These cells express a mutant form of SHP2, which contains the intact phosphatase domain, but target recognition is abolished. These cells showed intermediate CcO activities (increased by 37% compared to controls, Fig. 1B).

For all subsequent experiments we used MEF cell lines, because lymphoblasts contain fewer mitochondria and grow in clumps. In particular, separating cells from such cell aggregates, as required for some of the experiments shown below, triggers cell death.

3.2. Cytochrome c oxidase and cytochrome c levels are decreased in D61G cells

Increased CcO activity might be explained by increased CcO levels. We performed Western blot analysis for all OxPhos complexes and Cyt*c*, and porins, which are constituents of the outer mitochondrial membrane. Surprisingly, our results show that CcO was 37% reduced in D61G cells after normalization to GAPDH (Fig. 2). Interestingly, there was no significant

change in the protein levels of the other OxPhos complexes except Cyt*c* and porins that were decreased by 28% and 19% in D61G and increased by 25% and 15% in SHP2 knockdown cells (Fig. 2B). Since CcO amount is reduced in D61G cells and CcO activity is increased, data presented in Fig. 1, which are standardized to total protein, are an underestimation of CcO specific activity. Since increased CcO activity cannot be explained by concomitant changes in protein levels, alterations in posttranslational modifications may account for increased CcO activity. We have previously shown that phosphorylation of Y304 of CcO catalytic subunit I has a profound effect on CcO activity, such that phosphorylation leads to strong enzyme inhibition [17,18]. We have generated an antibody that specifically recognizes the pY304 epitope [17] and which, to our knowledge, is the only available antibody to a phosphoepitope mapped on CcO. We assessed possible changes in Y304 phosphorylation after 2D gel electrophoresis and Western analysis, but did not observe changes in subunit I Y304 phosphorylation (data not shown; see Discussion).

3.3. D61G cells have decreased citrate synthase activity, decreased ATP levels, and lower mitochondrial membrane potentials

Determination of citrate synthase (CS) activity, a marker of mitochondrial mass, revealed 17% and 24% decreased CS activity levels for D61G and SHP2 knockdown cells (Fig. 3A). Changes in mitochondrial mass and CcO activity (Fig. 1) may result in alterations in mitochondrial functionality. We first analyzed cellular energy levels in D61G cells and observed 33% lower ATP levels than in wild-type, whereas SHP2 knockdown cells showed a less dramatic decrease of 9% (Fig. 3B). The mitochondrial membrane potential $\Delta\Psi_m$ is the functional link between the proton pumps of the ETC and ATP synthase that utilizes the electrochemical gradient to produce ATP. We analyzed $\Delta\Psi_m$ with the membrane potential sensitive fluorescent probe TMRM by flow cytometry and normalized the resultant data to mitochondrial mass using the mitochondria-selective probe MitoTracker Red, which is not dependent on $\Delta\Psi_m$ in the three cell lines (data not shown). Strikingly, we observed a 61% reduction in TMRM fluorescence in D61G cells indicating a decreased $\Delta\Psi_m$ (Fig. 3C).

3.4. D61G cells show increased amounts of reactive oxygen species (ROS)

ROS cause cellular damage but also serve as signaling components. ROS have been implicated in numerous human diseases and can cause developmental abnormalities and therefore must be well regulated during gestation since they might otherwise interfere with organ development (see Discussion). We speculated that ROS may be altered in NS and analyzed ROS content using the ROS-sensitive probe CM-H_2DCFDA. Strikingly, fluorescence was 75% increased in D61G cells indicating increased ROS levels, whereas SHP2 knockdown cells show a 27% reduced fluorescent signal compared to controls (Fig. 4A).

3.5 Effect of SHP2 mutants on aconitase activity and radical scavenging enzymes

Increased ROS as observed in D61G cells are expected to cause cellular damage. Aconitase activity is a commonly used marker for ROS-induced damage, because it contains an enzymatically active $[Fe_4S_4]^{2+}$ cluster, which is highly sensitive to ROS. Aconitase catalyzes the conversion from citrate to isocitrate as part of the Krebs cycle and is located in the mitochondrial matrix. As expected, aconitase activity was 41% reduced in D61G cells. Surprisingly, SHP2 knockdown cells also showed, although less pronounced, 22% reduced aconitase activity (Fig. 4D).

As a possible consequence of increased ROS and ROS-induced damage in D61G cells, changes in cellular defense mechanisms, specifically ROS scavenging enzymes, may be expected. We analyzed four ROS scavengers. Protein levels of the cytosolic copper zinc superoxide dismutase (CuZnSOD) were similar in all three cell types (Fig. 4B and C). The mitochondrial manganese superoxide dismutase (MnSOD) is strongly upregulated in SHP2 knockdown cells

in contrast to D61G cells, and glutathione peroxidase levels are slightly increased in both cell types in comparison to controls (Fig. 4B and C). Catalase is another ROS scavenger mainly associated with peroxisomal degradation of H_2O_2. We found 28% increased catalase activity in D61G cells but no significant increase in SHP2 knockdown cells (Fig. 4E).

Discussion

Tyrosine phosphatase SHP2 might be a direct link between the MAPK pathway and OxPhos. Studies on rat brain, a tissue where SHP2 is expressed at high levels, showed partial localization of SHP2 to the mitochondrial IMS [9]. This localization makes the OxPhos complexes direct and indirect substrate candidates for SHP2. It is unclear how the MAPK pathway regulates mitochondrial function. However, there is evidence that it can affect OxPhos. For example, hearts of mice that overexpress MKK6, a p38 MAPK activator, showed reduced levels of all OxPhos complexes, reduced respiration rates and reduced ROS formation [30]. In contrast, we show here that human and mouse cells with constitutively active SHP2 have significantly increased CcO activities (Fig. 1), despite 37% reduced CcO levels (Fig. 2). Only the small electron carrier Cyt*c* showed a similar pattern with 28% reduced protein levels, whereas the other four OxPhos complexes were not significantly changed.

Considering reduced CcO levels in D61G cells, CcO activity reported in Fig. 1B is an underestimation of CcO specific activity in D61G cells. Normalization to GAPDH protein levels (Fig. 2) or citrate synthase activity (Fig. 3A) results in 2.7- and 2.3-fold increased CcO activity in D61G cells, respectively, compared to controls. Downregulation of CcO and Cyt*c* at the protein level may therefore reflect a compensatory mechanism for increased CcO specific activity. Therefore, our data suggests that the terminal step of the ETC, the electron transfer from Cyt*c* via CcO to molecular oxygen, is affected by SHP2 action.

In addition to the two tyrosine phosphorylation sites mapped on CcO, Y304 of catalytic subunit I and Y11 of regulatory subunit IV, several other serine and threonine sites have been mapped, which may be downstream indirect targets of SHP2. [31–34]. Perhaps, the most straightforward model of SHP2 action on CcO is to propose involvement of CcO subunit II phosphorylation by Src, which leads to an increase in CcO activity [29]. SHP2 is a positive regulator of Src, and *in vitro* is able to dephosphorylate Src residue Y527, a regulatory site located in the C-terminus region [35]. Later, an indirect mechanism was suggested to operate *in vivo* via protein-protein interactions [36]. Src also localizes to the IMS [37] and can possibly interact and thus be regulated by SHP2. Increased SHP2 activity would result in increased Src activity, an increase of CcO subunit II phosphorylation, and increased CcO activity. Once the phosphorylation site(s) on subunit II have been mapped and phosphoepitope-specific antibodies are in hand this model can stand trial.

Other signaling pathways, which have been shown to act on CcO without knowing the precise phosphorylation sites, may be affected by SHP2 signaling. These include PKC_{ε}, which was found to interact with CcO subunit IV by co-immunoprecipitation after stimulation of the signaling pathway followed by an increase in CcO activity [38,39]. Another candidate pathway is epidermal growth factor receptor (EGFR) signaling. After stimulation with EGF, EGFR was shown to translocate to the mitochondria and to interact with CcO subunit II [40].

Considering our finding of increased CcO activity together with a decreased mitochondrial membrane potential in D61G cells, one might speculate that dysregulated SHP2 activity has an effect on the proton pumping activity of the OxPhos complexes. Previously it was proposed that dephosphorylation of CcO could cause a “slip” of the proton pumping activity, i.e., a decreased H^+/e^- stoichiometry [41], leading to a decrease of the mitochondrial membrane potential and subsequently to reduced ATP production. Other mechanisms may be involved,

such as a proton slip in the other OxPhos complexes, or increased proton conductance mediated by uncoupling proteins in the inner mitochondrial membrane that have recently been shown to be regulated by phosphorylation [42]. Decreased mitochondrial membrane potential and ATP levels might also result from increased energy demand in D61G cells, perhaps due to an increased growth rate compared to the controls. In summary, the findings of decreased mitochondrial membrane potential and decreased cellular ATP levels strongly suggest an impairment of mitochondrial energy production.

The second pathological component associated with mitochondrial dysfunction in D61G cells is the significantly increased production of ROS. Generally, increased mitochondrial membrane potential levels are associated with increased ROS production (reviewed in [14]). However, decreased mitochondrial membrane potential levels in combination with increased mitochondrial ROS production have been described although the detailed mechanisms leading to increased ROS remain elusive. For example, hexavalent chromium, an inducer of apoptosis, was shown to trigger mitochondrial membrane potential depolarization in combination with increased ROS production [43]. The Avadhani group has recently shown in a mouse macrophage cell line that downregulation of CcO subunit Vb leads to decreased mitochondrial membrane potential levels in combination with increased ROS [44]. Our studies also consistently showed a decreased mitochondrial membrane potential but significantly increased ROS in D61G cells (Fig. 3C and 4A), which warrants further mechanistic studies. For example, it is possible that other OxPhos complexes show changes in their phosphorylation pattern, including complexes I and III, the main producers of ROS in the OxPhos system. The known increase of ROS caused by complex I and III inhibitors may be mimicked by (de-) phosphorylations of these complexes *in vivo*. On the other hand, a mitochondrial oxidative damage marker, aconitase activity, was not dramatically decreased in D61G cells when normalized to citrate synthase activity, and the decrease observed may not reflect the significant increase in ROS production via DCFDA fluorescence. Such increased ROS levels are rarely found in cells from patients with mitochondrial disorders with ROS involvement [45]. Therefore, an increase of non-mitochondrial ROS production cannot be ruled out.

Our unprecedented findings of decreased ATP levels and increased ROS may be important for a better understanding of the pathogenesis of some features observed in NS. ATP is required to drive all key cellular processes, and decreased energy levels can have a deleterious effect on human health and performance as can be seen in traditional mitochondrial diseases. These findings may explain, at least in part, the features of NS that overlap with children with a primary mitochondrial disorder including failure to thrive, hypotonia, developmental delays, short stature, ptosis, and hypertrophic cardiomyopathy. Furthermore, ROS play an important role in organ development including that of heart and brain. The participation of mitochondria in this process becomes evident after mid-gestation when most organs begin to grow to perform their adult function [46]. At this developmental stage a switching occurs from energy production that relies only 5% on aerobic metabolism before gestation day 9, to 95% after gestation day 11 as has been shown with cultured rat embryos [47]. Interestingly, fetal antioxidant activities such as superoxide dismutase are depressed until just prior to parturition [48], which might account for the increased capacity to generate ROS in fetal tissue [46]. The importance of a narrow window of ROS production for proper heart development and function was shown in a study using knockout mice lacking the mitochondrial thioredoxin reductase [49], leading to embryonic death after mid-gestation, when switching to aerobic metabolism takes place. Although crucial for organ development the amount of ROS must be well controlled. Relevant examples in this context are studies using streptozotocin-induced animal models for diabetes, where oxidative damage caused by ROS was found in fetuses of diabetic rats, leading to congenital abnormalities including anomalies of the heart and great vessels, and neuronal damage, which can in part be overcome by the application of high doses of antioxidants, such as vitamins C and E [50,51]. Better and more specific ROS scavengers have

been developed since then, which target ROS where they are produced. MitoQ, a ubiquinone derivative targeted to mitochondria by covalent attachment to the positively charged lipophilic triphenylphosphonium moiety [52] is now in clinical trial for Parkinson's disease [53]. Other slightly modified compounds including plastoquinonyl-decyl-triphenylphosphonium (SkQ1) were shown to have even better features such as increased anti-oxidant activities, require lower concentrations, and have produced remarkable results in several animal models of ROS-induced pathologies [54]. Applications of ROS scavengers to NS patients during pregnancy may be a future treatment to decrease congenital abnormalities.

Acknowledgments

The Center for Molecular Medicine and Genetics, and the Cardiovascular Research Institute Isis Initiative, Wayne State University School of Medicine, Detroit are gratefully acknowledged for supporting this work (MH). BGN is supported by grant R37 CA49132 and TA by a fellowship from the Leukemia and Lymphoma society. We thank Dr. Jeffrey W. Doan for suggestions on the manuscript. MH would also like to thank Dr. Katia Sol-Church, Ms. Lisa Schoyer, and Ms. Brenda Conger for insightful discussions.

Abbreviations

CcO	cytochrome *c* oxidase
Cyt*c*	cytochrome *c*
CS	citrate synthase
ETC	electron transport chain
IMS	intermembrane space
KD	knockdown
NS	Noonan syndrome
OxPhos	oxidative phosphorylation
WT	wild-type

References

1. Adachi M, Iwaki H, Shindoh M, Akao Y, Hachiya T, Ikeda M, Hinoda Y, Imai K. Predominant expression of the src homology 2-containing tyrosine phosphatase protein SHP2 in vascular smooth muscle cells. Virchows Arch 1997;430:321–325. [PubMed: 9134043]
2. Chong ZZ, Maiese K. The Src homology 2 domain tyrosine phosphatases SHP-1 and SHP-2: diversified control of cell growth, inflammation, and injury. Histol Histopathol 2007;22:1251–1267. [PubMed: 17647198]
3. Araki T, Nawa H, Neel BG. Tyrosyl phosphorylation of Shp2 is required for normal ERK activation in response to some, but not all, growth factors. J Biol Chem 2003;278:41677–41684. [PubMed: 12923167]
4. Saxton TM, Henkemeyer M, Gasca S, Shen R, Rossi DJ, Shalaby F, Feng GS, Pawson T. Abnormal mesoderm patterning in mouse embryos mutant for the SH2 tyrosine phosphatase Shp-2. Embo J 1997;16:2352–2364. [PubMed: 9171349]
5. Yang W, Klaman LD, Chen B, Araki T, Harada H, Thomas SM, George EL, Neel BG. An Shp2/SFK/Ras/Erk signaling pathway controls trophoblast stem cell survival. Dev Cell 2006;10:317–327. [PubMed: 16516835]
6. Keilhack H, David FS, McGregor M, Cantley LC, Neel BG. Diverse biochemical properties of Shp2 mutants. Implications for disease phenotypes. J Biol Chem 2005;280:30984–30993. [PubMed: 15987685]
7. Tartaglia M, Mehler EL, Goldberg R, Zampino G, Brunner HG, Kremer H, van der Burgt I, Crosby AH, Ion A, Jeffery S, Kalidas K, Patton MA, Kucherlapati RS, Gelb BD. Mutations in PTPN11,

encoding the protein tyrosine phosphatase SHP-2, cause Noonan syndrome. Nat Genet 2001;29:465–468. [PubMed: 11704759]

8. Roberts AE, Araki T, Swanson KD, Montgomery KT, Schiripo TA, Joshi VA, Li L, Yassin Y, Tamburino AM, Neel BG, Kucherlapati RS. Germline gain-of-function mutations in SOS1 cause Noonan syndrome. Nat Genet 2007;39:70–74. [PubMed: 17143285]
9. Salvi M, Stringaro A, Brunati AM, Agostinelli E, Arancia G, Clari G, Toninello A. Tyrosine phosphatase activity in mitochondria: presence of Shp-2 phosphatase in mitochondria. Cell Mol Life Sci 2004;61:2393–2404. [PubMed: 15378208]
10. Arachiche A, Augereau O, Decossas M, Pertuiset C, Gontier E, Letellier T, Dachary-Prigent J. Localization of PTP-1B, SHP-2, and Src exclusively in rat brain mitochondria and functional consequences. J Biol Chem 2008;283:24406–24411. [PubMed: 18583343]
11. Kadenbach B, Ramzan R, Vogt S. Degenerative diseases, oxidative stress and cytochrome c oxidase function. Trends Mol Med 2009;15:139–147. [PubMed: 19303362]
12. Liu SS. Cooperation of a “reactive oxygen cycle” with the Q cycle and the proton cycle in the respiratory chain--superoxide generating and cycling mechanisms in mitochondria. J Bioenerg Biomembr 1999;31:367–376. [PubMed: 10665526]
13. Huttemann M, Lee I, Samavati L, Yu H, Doan JW. Regulation of mitochondrial oxidative phosphorylation through cell signaling. Biochim Biophys Acta 2007;1773:1701–1720. [PubMed: 18240421]
14. Huttemann M, Lee I, Pecinova A, Pecina P, Przyklenk K, Doan JW. Regulation of oxidative phosphorylation, the mitochondrial membrane potential, and their role in human disease. J Bioenerg Biomembr 2008;40:445–456. [PubMed: 18843528]
15. Ko YH, Pan W, Inoue C, Pedersen PL. Signal transduction to mitochondrial ATP synthase: evidence that PDGF-dependent phosphorylation of the delta-subunit occurs in several cell lines, involves tyrosine, and is modulated by lysophosphatidic acid. Mitochondrion 2002;1:339–348. [PubMed: 16120288]
16. Lee I, Salomon AR, Yu K, Samavati L, Pecina P, Pecinova A, Huttemann M. Isolation of regulatory-competent, phosphorylated cytochrome *c* oxidase. Methods Enzymol 2009;457:193–210. [PubMed: 19426869]
17. Samavati L, Lee I, Mathes I, Lottspeich F, Huttemann M. Tumor necrosis factor α inhibits oxidative phosphorylation through tyrosine phosphorylation at subunit I of cytochrome *c* oxidase. J Biol Chem 2008;283:21134–21144. [PubMed: 18534980]
18. Lee I, Salomon AR, Ficarro S, Mathes I, Lottspeich F, Grossman LI, Huttemann M. cAMP-dependent tyrosine phosphorylation of subunit I inhibits cytochrome c oxidase activity. J Biol Chem 2005;280:6094–6100. [PubMed: 15557277]
19. Lee I, Salomon AR, Yu K, Doan JW, Grossman LI, Huttemann M. New prospects for an old enzyme: mammalian cytochrome c is tyrosine-phosphorylated in vivo. Biochemistry 2006;45:9121–9128. [PubMed: 16866357]
20. Yu H, Lee I, Salomon AR, Yu K, Huttemann M. Mammalian liver cytochrome c is tyrosine-48 phosphorylated in vivo, inhibiting mitochondrial respiration. Biochim Biophys Acta 2008;1777:1066–1071. [PubMed: 18471988]
21. Araki T, Mohi MG, Ismat FA, Bronson RT, Williams IR, Kutok JL, Yang W, Pao LI, Gilliland DG, Epstein JA, Neel BG. Mouse model of Noonan syndrome reveals cell type- and gene dosage-dependent effects of Ptpn11 mutation. Nat Med 2004;10:849–857. [PubMed: 15273746]
22. Oh ES, Gu H, Saxton TM, Timms JF, Hausdorff S, Frevert EU, Kahn BB, Pawson T, Neel BG, Thomas SM. Regulation of early events in integrin signaling by protein tyrosine phosphatase SHP-2. Mol Cell Biol 1999;19:3205–3215. [PubMed: 10082587]
23. Zhang SQ, Tsiaras WG, Araki T, Wen G, Minichiello L, Klein R, Neel BG. Receptor-specific regulation of phosphatidylinositol 3′-kinase activation by the protein tyrosine phosphatase Shp2. Mol Cell Biol 2002;22:4062–4072. [PubMed: 12024020]
24. Plasek J, Vojtiskova A, Houstek J. Flow-cytometric monitoring of mitochondrial depolarisation: from fluorescence intensities to millivolts. J Photochem Photobiol B 2005;78:99–108. [PubMed: 15664496]

25. Chowdhury SK, Drahota Z, Floryk D, Calda P, Houstek J. Activities of mitochondrial oxidative phosphorylation enzymes in cultured amniocytes. Clin Chim Acta 2000;298:157–173. [PubMed: 10876012]
26. Acsadi G, Lee I, Li X, Khaidakov M, Pecinova A, Parker G, Huttemann M. Mitochondrial dysfunction in a neural cell model of spinal muscular atrophy. J Neurosci Res 2009;87:2748–56. [PubMed: 19437551]
27. Bulteau AL, Ikeda-Saito M, Szweda LI. Redox-dependent modulation of aconitase activity in intact mitochondria. Biochemistry 2003;42:14846–14855. [PubMed: 14674759]
28. Beers RF Jr, Sizer IW. A spectrophotometric method for measuring the breakdown of hydrogen peroxide by catalase. J Biol Chem 1952;195:133–140. [PubMed: 14938361]
29. Miyazaki T, Neff L, Tanaka S, Horne WC, Baron R. Regulation of cytochrome c oxidase activity by c-Src in osteoclasts. J Cell Biol 2003;160:709–718. [PubMed: 12615910]
30. Wall JA, Wei J, Ly M, Belmont P, Martindale JJ, Tran D, Sun J, Chen WJ, Yu W, Oeller P, Briggs S, Gustafsson AB, Sayen MR, Gottlieb RA, Glembotski CC. Alterations in oxidative phosphorylation complex proteins in the hearts of transgenic mice that overexpress the p38 MAP kinase activator, MAP kinase kinase 6. Am J Physiol Heart Circ Physiol 2006;291:H2462–2472. [PubMed: 16766635]
31. Tsukihara T, Shimokata K, Katayama Y, Shimada H, Muramoto K, Aoyama H, Mochizuki M, Shinzawa-Itoh K, Yamashita E, Yao M, Ishimura Y, Yoshikawa S. The low-spin heme of cytochrome c oxidase as the driving element of the proton-pumping process. Proc Natl Acad Sci U S A 2003;100:15304–15309. [PubMed: 14673090]
32. Helling S, Vogt S, Rhiel A, Ramzan R, Wen L, Marcus K, Kadenbach B. Phosphorylation and kinetics of mammalian cytochrome c oxidase. Mol Cell Proteomics 2008;7:1714–1724. [PubMed: 18541608]
33. Prabu SK, Anandatheerthavarada HK, Raza H, Srinivasan S, Spear JF, Avadhani NG. Protein kinase A-mediated phosphorylation modulates cytochrome c oxidase function and augments hypoxia and myocardial ischemia-related injury. J Biol Chem 2006;281:2061–2070. [PubMed: 16303765]
34. Fang JK, Prabu SK, Sepuri NB, Raza H, Anandatheerthavarada HK, Galati D, Spear J, Avadhani NG. Site specific phosphorylation of cytochrome *c* oxidase subunits I, IVi1 and Vb in rabbit hearts subjected to ischemia/reperfusion. FEBS Lett 2007;581:1302–1310. [PubMed: 17349628]
35. Peng ZY, Cartwright CA. Regulation of the Src tyrosine kinase and Syp tyrosine phosphatase by their cellular association. Oncogene 1995;11:1955–1962. [PubMed: 7478513]
36. Walter AO, Peng ZY, Cartwright CA. The Shp-2 tyrosine phosphatase activates the Src tyrosine kinase by a non-enzymatic mechanism. Oncogene 1999;18:1911–1920. [PubMed: 10208413]
37. Salvi M, Brunati AM, Bordin L, La Rocca N, Clari G, Toninello A. Characterization and location of Src-dependent tyrosine phosphorylation in rat brain mitochondria. Biochim Biophys Acta 2002;1589:181–195. [PubMed: 12007793]
38. Ogbi M, Johnson JA. Protein kinase Cepsilon interacts with cytochrome c oxidase subunit IV and enhances cytochrome c oxidase activity in neonatal cardiac myocyte preconditioning. Biochem J 2006;393:191–199. [PubMed: 16336199]
39. Ogbi M, Chew CS, Pohl J, Stuchlik O, Ogbi S, Johnson JA. Cytochrome c oxidase subunit IV as a marker of protein kinase Cepsilon function in neonatal cardiac myocytes: implications for cytochrome c oxidase activity. Biochem J 2004;382:923–932. [PubMed: 15339253]
40. Boerner JL, Demory ML, Silva C, Parsons SJ. Phosphorylation of Y845 on the epidermal growth factor receptor mediates binding to the mitochondrial protein cytochrome c oxidase subunit II. Mol Cell Biol 2004;24:7059–7071. [PubMed: 15282306]
41. Kadenbach B. Intrinsic and extrinsic uncoupling of oxidative phosphorylation. Biochim Biophys Acta 2003;1604:77–94. [PubMed: 12765765]
42. Carroll AM, Porter RK, Morrice NA. Identification of serine phosphorylation in mitochondrial uncoupling protein 1. Biochim Biophys Acta 2008;1777:1060–1065. [PubMed: 18486593]
43. Hayashi Y, Kondo T, Zhao QL, Ogawa R, Cui ZG, Feril LB Jr, Teranishi H, Kasuya M. Signal transduction of p53-independent apoptotic pathway induced by hexavalent chromium in U937 cells. Toxicol Appl Pharmacol 2004;197:96–106. [PubMed: 15163545]
44. Galati D, Srinivasan S, Raza H, Prabu SK, Hardy M, Chandran K, Lopez M, Kalyanaraman B, Avadhani NG. Role of nuclear-encoded subunit Vb in the assembly and stability of cytochrome c

oxidase complex: implications in mitochondrial dysfunction and ROS production. Biochem J 2009;420:439–449. [PubMed: 19338496]

45. Baracca A, Sgarbi G, Mattiazzi M, Casalena G, Pagnotta E, Valentino ML, Moggio M, Lenaz G, Carelli V, Solaini G. Biochemical phenotypes associated with the mitochondrial ATP6 gene mutations at nt8993. Biochim Biophys Acta 2007;1767:913–919. [PubMed: 17568559]
46. Fantel AG, Person RE. Involvement of mitochondria and other free radical sources in normal and abnormal fetal development. Ann N Y Acad Sci 2002;959:424–433. [PubMed: 11976215]
47. Morriss GM, New DA. Effect of oxygen concentration on morphogenesis of cranial neural folds and neural crest in cultured rat embryos. J Embryol Exp Morphol 1979;54:17–35. [PubMed: 528863]
48. Mackler B, Person RE, Nguyen TD, Fantel AG. Studies of the cellular distribution of superoxide dismutases in adult and fetal rat tissues. Free Radic Res 1998;28:125–129. [PubMed: 9645389]
49. Conrad M, Jakupoglu C, Moreno SG, Lippl S, Banjac A, Schneider M, Beck H, Hatzopoulos AK, Just U, Sinowatz F, Schmahl W, Chien KR, Wurst W, Bornkamm GW, Brielmeier M. Essential role for mitochondrial thioredoxin reductase in hematopoiesis, heart development, and heart function. Mol Cell Biol 2004;24:9414–9423. [PubMed: 15485910]
50. Siman CM, Eriksson UJ. Vitamin C supplementation of the maternal diet reduces the rate of malformation in the offspring of diabetic rats. Diabetologia 1997;40:1416–1424. [PubMed: 9447949]
51. Siman M. Congenital malformations in experimental diabetic pregnancy: aetiology and antioxidative treatment. Minireview based on a doctoral thesis. Ups J Med Sci 1997;102:61–98. [PubMed: 9394431]
52. Kelso GF, Porteous CM, Coulter CV, Hughes G, Porteous WK, Ledgerwood EC, Smith RA, Murphy MP. Selective targeting of a redox-active ubiquinone to mitochondria within cells: antioxidant and antiapoptotic properties. J Biol Chem 2001;276:4588–4596. [PubMed: 11092892]
53. Tauskela JS. MitoQ--a mitochondria-targeted antioxidant. IDrugs 2007;10:399–412. [PubMed: 17642004]
54. Skulachev VP. A biochemical approach to the problem of aging: “megaproject” on membrane-penetrating ions. The first results and prospects. Biochemistry (Mosc) 2007;72:1385–1396. [PubMed: 18205623]
55. Osheroff N, Speck SH, Margoliash E, Veerman EC, Wilms J, Konig BW, Muijsers AO. The reaction of primate cytochromes c with cytochrome c oxidase. Analysis of the polarographic assay. J Biol Chem 1983;258:5731–5738. [PubMed: 6304097]

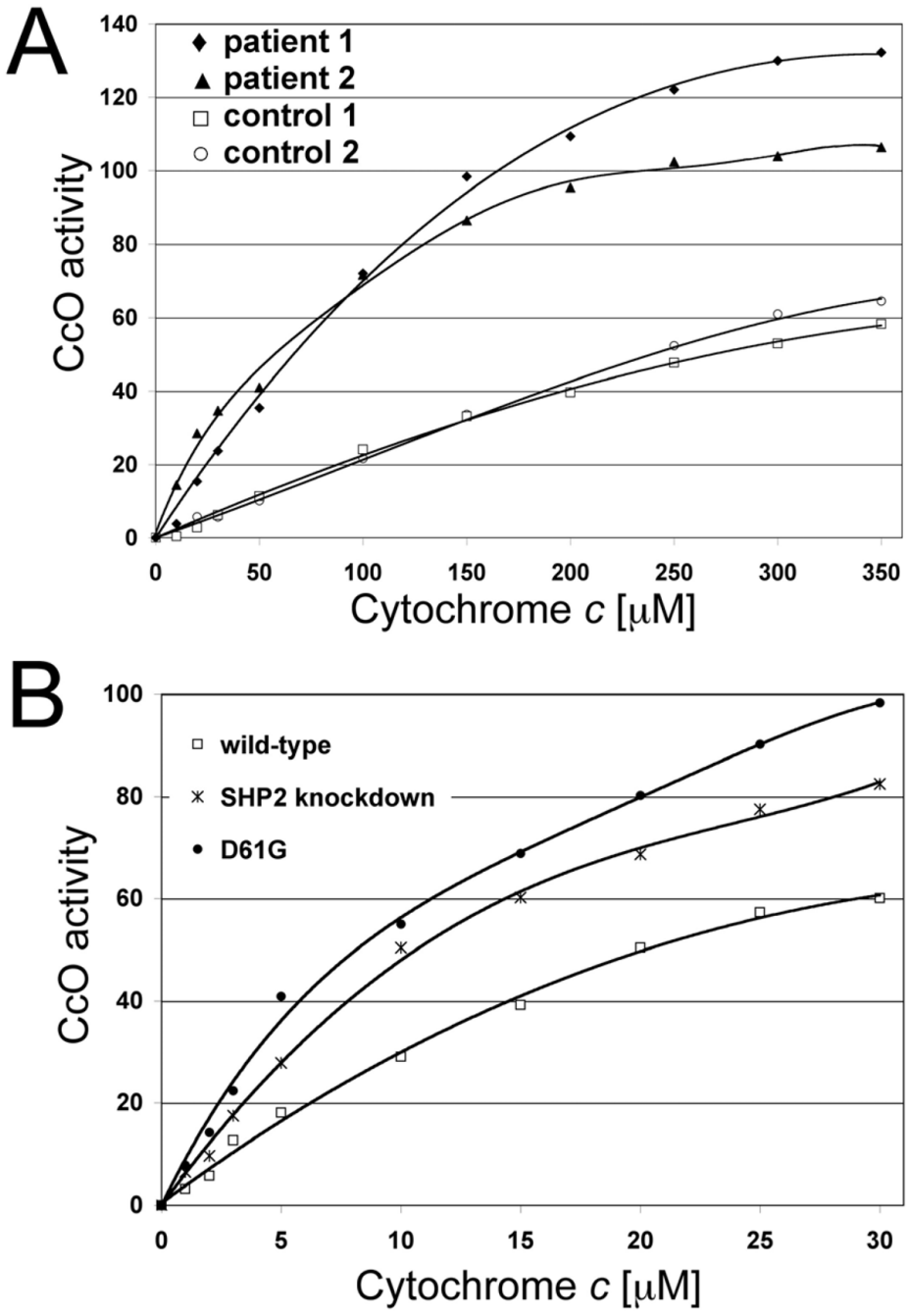

Fig. 1.

Cytochrome *c* oxidase activity is increased in Noonan syndrome cell lines. (A) CcO activity of cell homogenates of lymphoblast cell lines from Noonan patients (patient 1, ◆: A317C (Asp106Ala); patient 2, ▲: A922G (Asn308Asp) and controls (open symbols, □ and ○) was analyzed with the polarographic method by increasing the amount of substrate cytochrome *c*. (B) CcO activity of mouse fibroblast cell lines from control (□), SHP2 knockdown (*), and Asp61Gly (●), a mutation found in Noonan patients. CcO activity is defined as consumed O_2 [μM]/min/protein [mg]. Shown are representative measurements for each cell line (3 replicates each, analyzed on the same day; standard deviation <4% at maximal turnover).

Higher amounts of cow cytochrome *c* are necessary to stimulate human CcO (A) compared to mouse CcO (B) as a result of the imperfect match [55].

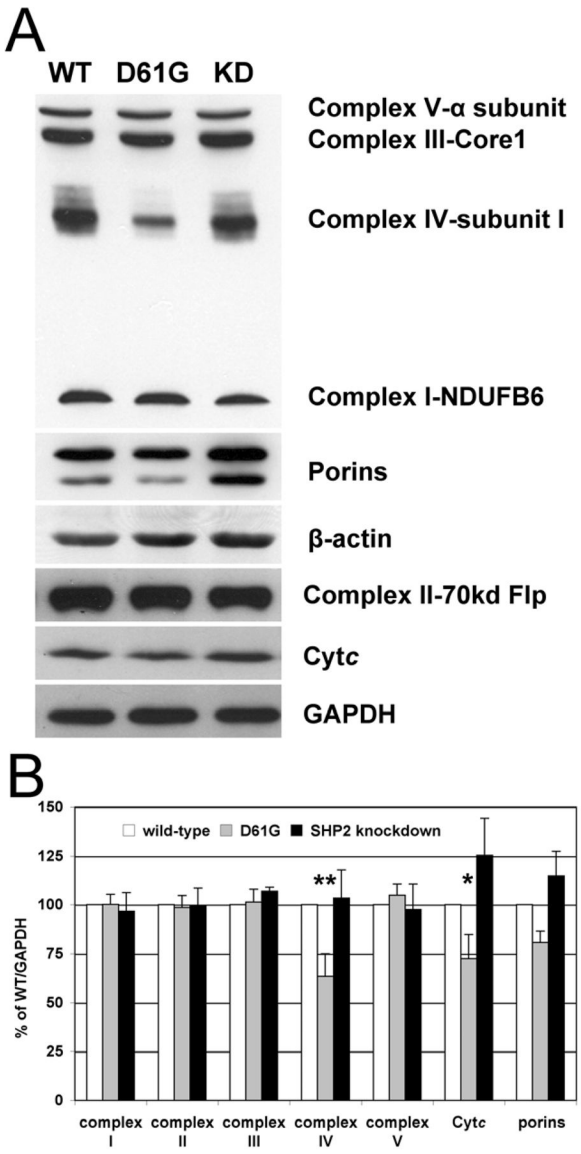

Fig. 2.

Expression analysis of OxPhos complexes and cytochrome *c*. (A) Western blot analysis of primary antibodies were as follows. Complex I: anti-NDUFB6, complex II: anti-70kd flavoprotein, complex III: anti-core I, complex IV: anti-subunit I, complex V: anti-α subunit, GAPDH: glyceraldehyde 3-phosphate dehydrogenase. (B) Quantitative assessment of protein levels by densitometric analysis of Western blots normalized to GAPDH (n = 3). Among OxPhos components, CcO and Cyt*c* levels are 37% ($p<0.02$, **) and 28% ($p=0.05$, *) reduced in D61G cells.

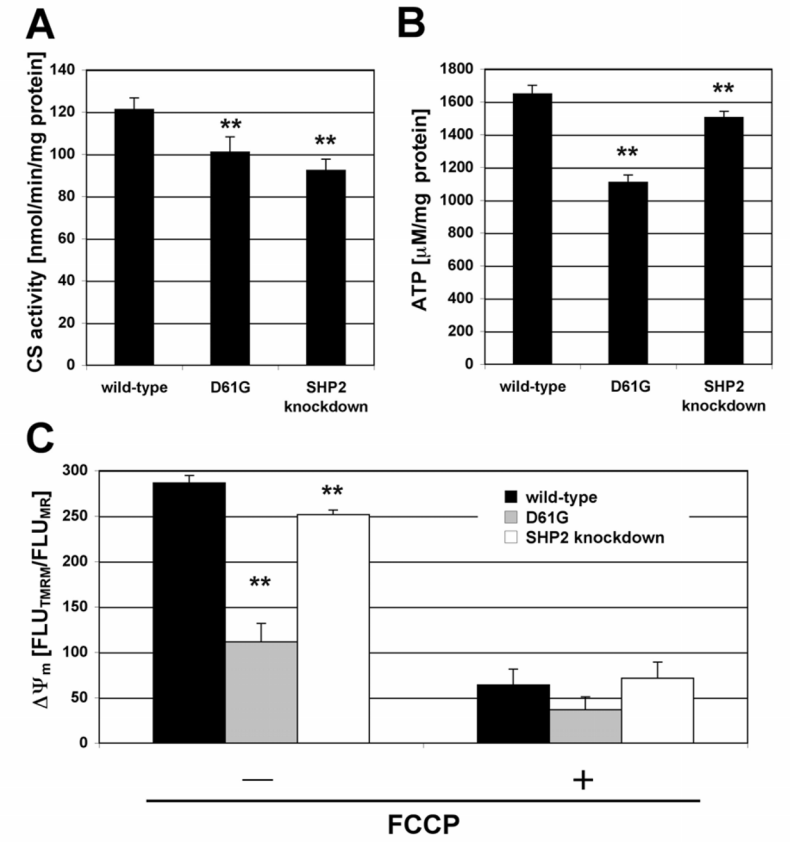

Fig. 3.

(A) Citrate synthase (CS) activity measurements. Solubilized cells were incubated with oxaloacetate, acetyl coA, and DTNB (5′-dithiobis-(2-nitrobenzoic acid)). Production of CoA-DTNB was detected at 420 nm spectrophotometrically. CS activity was 17% and 24% reduced in D61G and SHP2 knockdown cells compared to controls (n=3; $p<0.005$, **). (B) ATP content was determined with the bioluminescent method and were 33% and 9% reduced in D61G and SHP2 knockdown cells (n=3; $p<0.0001$, **). (C) Mitochondrial membrane potential measurements using TMRM via flow cytometry analysis (n=4). TMRM fluorescence was normalized to Mitotracker red fluorescence, which is a membrane potential independent mitochondrial marker in these cells. D61G cells show a 61% reduction in fluorescent signal compared to controls indicating decreased ΔΨm levels ($p<0.0001$, **).

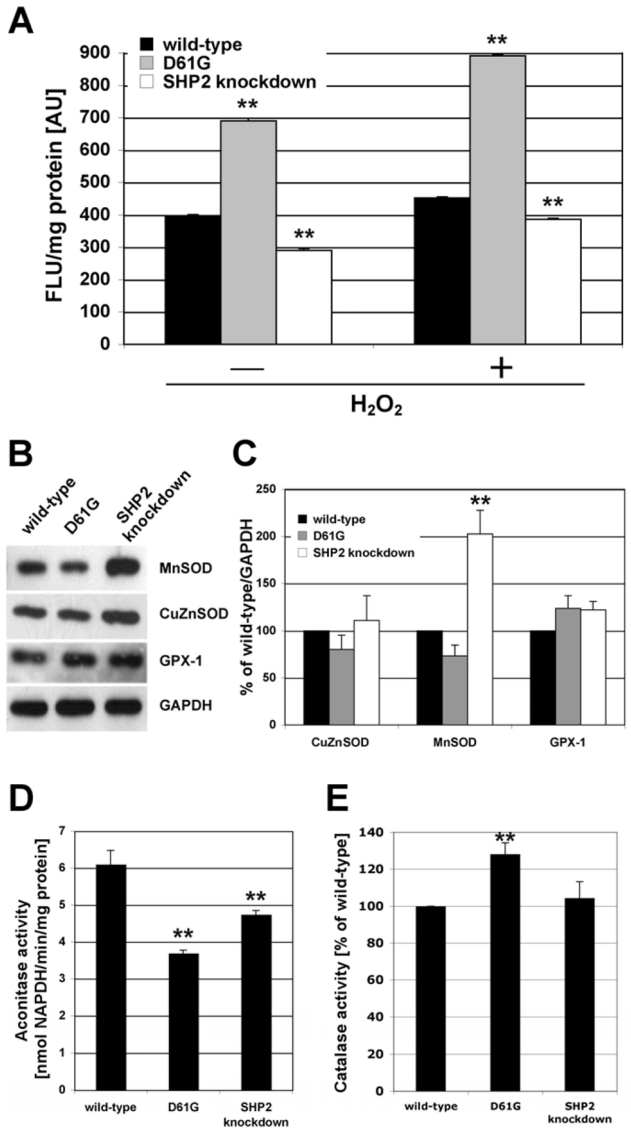

Fig. 4.

(A) Reactive oxygen species (ROS) were measured using the probe 5-(and-6)-chloromethyl-2′, 7′-dichlorodihydrofluorescein diacetate acetyl ester (CM-H_2DCFDA). Compared to controls, D61G cells show a 75% increased fluorescence indicating significantly increased ROS levels whereas SHP2 knockdown cells showed a 27% decreased signal (n=3; $p \ll 0.0001$, **). As a positive control, 100 μM H_2O_2 were added to the cells. (B) Western blot analysis of superoxide dismutases (MnSOD and CuZnSOD) and glutathione peroxidase 1 (GPX-1). (C) Quantitative representation of data presented in (B). MnSOD, CuZnSOD, and GPX-1 protein levels were normalized to GAPDH. Changes in protein levels in D61G cells were not significant. MnSOD levels in SHP2 knockdown cells were increased twofold ($p<0.001$, **). (D) Aconitase activity measurements revealed 41% and 22% reduced activities in D61G and SHP2 knockdown cells compared to controls (n=3; $p<0.0001$, **). (E) Catalase activity measurements showing 28% increased activity in D61G cells compared to controls (n=3; $p<0.01$, **).